

# RF-Pen: Practical Real-Time RFID Tracking in the Air

Haoyu Wang<sup>1</sup> and Wei Gong<sup>1</sup>, *Member, IEEE*

**Abstract**—Wireless tracing technologies have seen great potentials in many applications, including drawing and writing, gesture-based commanding, and gaming. Many state-of-the-art systems have recently been proposed along this line. However, none of them can strike a balance among hardware complexity, time delay, and accuracy in real-world scenarios. In this paper, we propose RF-Pen, a practical and complete RFID tracking system that achieves centimeter-level real-time tracing with 4 antennas. To do so, RF-Pen mainly employs two key designs, namely selective hologram and hybrid voting. Our selective hologram places antennas in large separation, which not only expedites the tracking process by producing a handful of good-quality candidate points but also maximizes tracing resolution. Nevertheless, a big challenge is ambiguity. To address this, we introduce hybrid voting that effectively integrates RSSI and phase measurements to evaluate the likelihood of all candidate points. This way, a precise initial position and fine-resolution tracing beams are located. We implement RF-Pen using off-the-shelf readers and tags and compare it against state-of-the-art systems. Results show that with a single reader of 4 antennas, RF-pen achieves a median trajectory error of 2.15 cm and a median position error of 12.8 cm, which are 3.7 $\times$  and 4.1 $\times$  better than RF-IDraw, respectively.

**Index Terms**—RFID, antenna array, real-time tracking

## 1 INTRODUCTION

RECENTLY, RF-tracking has attract much attention from both the industry and research community as it benefits more and more applications in human-computer interaction [1], business analytics [2] and smart homes [3]. Ideal indoor RF-tracking systems, particularly for RFIDs, should satisfy the following four requirements:

- *Complete.* They should have two integral parts: initial position estimation and trajectory tracing. Besides the tracing resolution, initial position error determines how accurate a trajectory could be. So, a complete tracking system should be able to provide precise initial position estimations and fine-resolution tracing services at the same time.
- *Accurate.* They should be as accurate as other RFID-based systems. To the best of our knowledge, state-of-the-art systems achieve 3-10 cm median trajectory errors, as shown in Table 1. Hence comparable or even better accuracy would be our design target. Note that this includes systems that may use extra resources, e.g., RF-IDraw can achieve 3.7 cm median trajectory error using 2 readers and 8 antennas.
- *Fast.* As many tracing-based applications are time sensitive, such as gaming and drawing, time delay on the order of seconds would be considered unfit. Therefore, a real-time tracking system should try to

reduce all possible delays, including hardware turn-about, tag reading, and computation overhead.

- *Cost-effective.* In many occasions, more hardware can bring better performance but usually comes at a higher cost. High-cost solutions are not scalable and thus hard to deploy in practice. A practical RF-tracking system should achieve the same or better accuracy without increasing hardware cost.

The above four requirements seem simple but hard to realize at the same time in practice. The first complete RFID tracing system, RF-IDraw is proposed in [4]. It designs a multi-resolution scheme that achieves a 3.7 cm median tracing error and a 19 cm median position error using 2 readers and 8 antennas. As it involves too much hardware, [5] introduces a simplified 4-antenna version of RF-IDraw. Nevertheless, this 4-antenna version's tracing error and position error degrade to 8 cm and 53 cm. Tagoram [6] is an accurate tracing system mainly designed for known tracks and works not so well with unknown tracks. But in most real-world applications like writing and drawing, the trajectory is unknown in advance, so for fair comparison, we mainly discuss its unknown track version here. The main drawback of Tagoram is the long time delay, which is more than 2.5 s. Such high delay is associated with its brute-force search design and thus hard to optimize. PolarDraw [5] presents how to use polarization to assist tracing and reduce the required no. of antennas from 4 to 2. However, such a 2-antenna design cannot do initial position estimation. Thus, it randomly chooses the starting point on hyperbolas, which will inevitably increase tracing error to 10.4 cm.

With all the above goals in mind, we present RF-Pen, a practical and complete RF tracking system that achieves centimeter-level real-time tracing with 4 antennas. It delivers the most accurate real-time positioning and tracing services

• The authors are with the School of Computer Science and Technology, University of Science and Technology of China, Hefei 230052, China.  
E-mail: tzwhy@mail.ustc.edu.cn, weigong@ustc.edu.cn.

Manuscript received 13 Aug. 2019; revised 7 Apr. 2020; accepted 20 May 2020.  
Date of publication 25 May 2020; date of current version 1 Oct. 2021.

(Corresponding author: Wei Gong.)

Digital Object Identifier no. 10.1109/TMC.2020.2997080

TABLE 1  
Comparison of RF-Pen Against State-of-the-Art Systems

	Median trajectory error (cm)	Median position error (cm)	Time delay	No. of readers	No. of antennas	COTS device
RF-Pen	2.15	12.8	~ ms	1	4	Yes
RF-IDraw (8-antenna) [4]	3.7	19	~ ms	2	8	Yes
RF-IDraw (4-antenna) [5]	8.0	53	~ ms	1	4	Yes
Tagoram (Unknown track) [6]	12.3	N/A	$\geq 2.5$ s	1	4	Yes
PolarDraw [5]	10.4	N/A	~ ms	1	2	Yes
RFind [7]	$\geq 10$	0.92	6.4s	2	2	No
TurboTrack [8]	0.9	0.51	~ms	4	5	No

\* As the table shows, only RF-pen and RF-IDraw are complete systems based on COTS devices that can provide initial position estimations and trajectory tracing at the same time. The time delay of Tagoram is far away from real-time that tracing applications require. While PolarDraw may use fewer hardware resources than other systems, its accuracy is not satisfied - decimeter-level. Considering completeness of systems, hardware complexity, time delay, and accuracy, RF-Pen achieves the best balance among all state-of-the-art systems.

among all the state-of-the-art systems using comparable hardware. We design RF-pen based on a key observation that tracing accuracy mainly depends on tracing resolution and initial position error. So we first design selective hologram with large antenna-separation. Using the antenna pair with wide separation, we can obtain a family of fine-resolution hyperbolas. Thus, by intersecting the hyperbolas at the mutually perpendicular directions, RF-Pen generates a handful of candidate points. While our selective hologram guarantees fine tracing resolution, it inevitably introduces ambiguity among all the candidate points and affects initial position error significantly. To address this, unlike previous systems, e.g., RF-IDraw, choose to use more antenna pairs and readers, we novelly introduce hybrid voting that integrates both Received Signal Strength Indicator(RSSI) and phase measurements together to estimate the initial position. Also, we take care of a number of measurement errors brought by noise and antenna diversity.

We implement RF-Pen with a ThingMagic M6e reader of 4 antennas. Extensive experiments are done to evaluate and compare it against state-of-the-art systems. Our results show that RF-pen achieves a median initial position error of 12.8 cm, which is  $4.1\times$  and  $1.5\times$  more accurate than RF-IDraw with 4 antennas and 8 antennas, respectively. For trajectory accuracy, RF-Pen achieves a median trajectory error of 2.15 cm, which is  $3.7\times$  and  $1.7\times$  better than RF-IDraw with 4 antennas and 8 antennas. Furthermore, RF-Pen is able to do character recognition at 97.9 percent success rate. A sample tracing result is shown in Fig. 1.

*Contribution.*

- We discover that the trajectory accuracy is positively correlated with initial position accuracy. Based on this observation, we design a new hybrid method for initial position estimation by combining phase and RSSI.

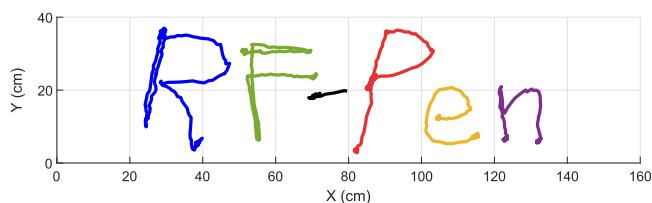


Fig. 1. Reconstructed trajectory of characters 'R', 'F', '-', 'P', 'e', 'n' by RF-Pen.

- We implement a RFID tracking system named RF-Pen. To the best of our knowledge, RF-Pen is the first complete RF-tracking system based on COTS devices that achieves 2.15 cm tracing error using only 4 antennas in real-time.
- We compare RF-Pen with some state-of-art systems. With a single reader and 4 antennas, RF-Pen is  $4.1\times$  and  $3.7\times$  better than RF-IDraw in initial positioning and tracing.

## 2 MOTIVATION

A complete tracking system is composed of two main parts, initial position estimation and trajectory tracing [4]. And RF-Pen is mainly motivated by an observation that tracing accuracy is significantly influenced by initial position error and tracing resolution. First, let's see how initial position estimations affect tracing. As shown in Fig. 2a, when initial position difference is large, trajectory accuracy degrades. If the starting points are close, as shown in Fig. 2b, trajectory shapes exhibit significant similarity. Hence, if we can make initial position estimations as accurate as possible, so is trajectory tracing.

Furthermore, we learned an important aspect of antenna arrays from our experiments and RF-IDraw: Antenna pairs with large separation have many very narrow beams (fine-resolution) while pairs with small separation have a single thick beam. The blue lines in Fig. 3b are beams emitted by the large-separation pair, and the yellow one is beam emitted by the narrow-separation pair. Note that the downside of large separation is ambiguity.

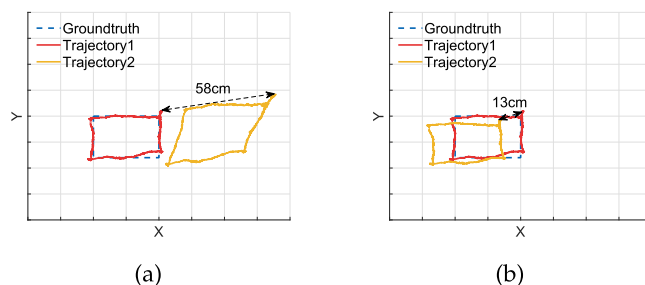


Fig. 2. Tracing comparison of different initial positions: The difference of two trajectories (a) with far-away initial positions (58 cm from each other) is much more significant than that of two trajectories (b) with two close starting points. Therefore, the more accurate initial positions, the more precise trajectories.

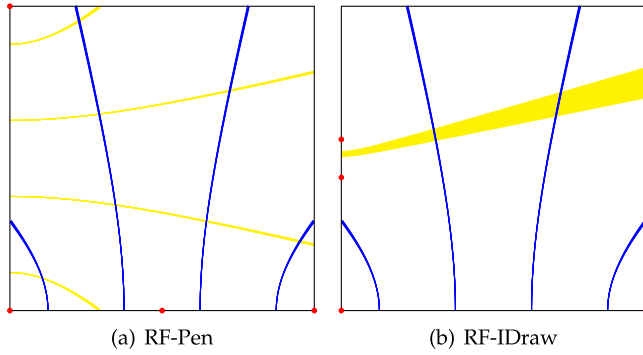


Fig. 3. *Antenna placement comparison*: This figure is a schematic diagram of obtaining candidate points. A red dot symbols an antenna. In reality, there will be much more candidate points than shown. (a) On each side, the antenna pair with wide separation will produce many hyperbolae (The middle antenna doesn't function at this stage). The intersections of blue and yellow hyperbolae are candidate points. (b) It's like RF-Pen in the horizontal direction, but only one thick hyperbola will be emitted from the narrow pair in the vertical direction. Therefore, RF-IDraw has a lower resolution, which, even worse, leads to a larger trajectory error in tracing stage.

Now we ask ourselves a question: is it possible to keep fine resolution and remove ambiguity without introducing more hardware? Fortunately, RF-Pen gives a very positive answer. Specifically, RF-Pen introduces selective hologram to make resolution fine enough and generate a handful of candidate points. Then it uses hybrid voting to remove ambiguity, which is quite different from RF-IDraw that mainly relies on more antenna pairs.

### 3 SELECTIVE HOLOGRAM

The design goal of selective hologram is to generate fine-resolution tracing candidates. So we first start with beam generation model and then present our antenna placement to compute selective hologram.

#### 3.1 Beam Generation

In RFID systems, the battery-free tags backscatter the wireless signal from the reader's antenna. Therefore, tags are usually attached to the object being tracking. By reading the backscatter signal, we can track the object accurately.

Phase is a parameter universally supported by RFID systems. According to physics, when an electromagnetic wave travels a distance of wavelength, its phase rotates  $2\pi$ . In fact, the reader cannot tell if a signal is rotated  $\phi_x$  or  $\phi_x + \pi$ , as it only returns values between 0 and  $\pi$ , which makes the phase look like being wrapped. Simply, considering that the wave propagates back and forth, we can express the phase as

$$\phi = \left( -\frac{2d}{\lambda} \times 2\pi \right) \bmod \pi, \quad (1)$$

where  $\lambda$  is the wavelength and  $d$  is the antenna-tag distance. In RF positioning, it's common to derive the direction of positions by comparing the phase differences of multiple antennas. Fig. 4 shows such a model. A and B are two antennas, and S is a tag. Both A and B are able to receive the signal backscattered by S. The difference between  $\phi_A$  and  $\phi_B$  can be expressed as

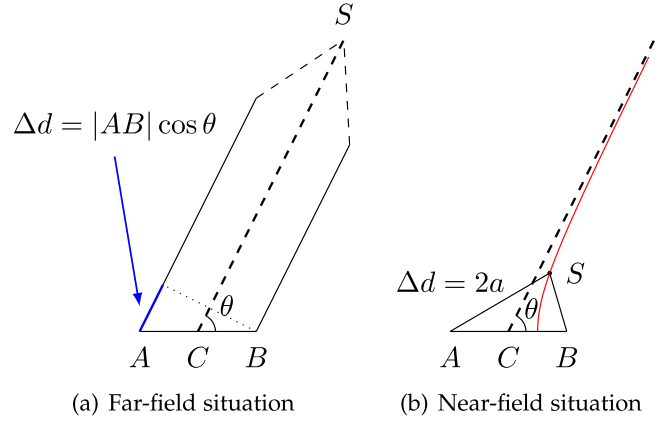


Fig. 4. *Beam generation models*: (a) If the tag is far away from the antenna pair, the paths from A to S and from B to S can be approximated as parallel. We can get  $\theta$  from  $\Delta d$  and locate the tag on the ray from C, the midpoint of AB. (b) Normally, the tag can be located on a hyperbola whose focuses are A and B. Its argument  $a$  can be calculated from  $\Delta d$ . It's obvious that there is a non-negligible gap between hyperbola and ray when the tag is near the antennas. In fact, the ray mentioned above is the asymptote of the hyperbola.

$$\phi_A - \phi_B \equiv 4\pi \frac{|SB| - |SA|}{\lambda} \bmod \pi. \quad (2)$$

Therefore, we get the relationship between phase difference and distance difference. Let  $D = |AB|$ ,  $\Delta d = |SB| - |SA|$ ,  $\Delta\phi = \phi_A - \phi_B$ . Considering the geometric relationship  $|\Delta d| < D$ , we can transform Equation (2) into

$$\begin{aligned} \Delta d &= \left( \frac{\Delta\phi}{4\pi} + \frac{k}{4} \right) \lambda \\ k &\in \left( -\frac{4D}{\lambda} - \frac{\Delta\phi}{\pi}, \frac{4D}{\lambda} - \frac{\Delta\phi}{\pi} \right) \cap \mathbb{Z}. \end{aligned} \quad (3)$$

First, let's consider a special case. If S is far from A and B, then  $\Delta d$  can be approximated as  $|AB| \cdot \cos\theta$ . Easily, we can get a new equation as

$$\cos\theta = \left( \frac{\Delta\phi}{4\pi} + \frac{k}{4} \right) \frac{\lambda}{D}. \quad (4)$$

For  $D = m\lambda$ , there are  $8m$  different possible values of  $k$  that satisfy Equation (4). Thus, these  $8m$  different rays emitted from C, the midpoint of AB, are all possible positions of S. As D increases, the number of rays increases with rising ambiguity, which seems to be detrimental to positioning. At the same time, however, the resolution is improving.

Now, we can regard the phase difference as  $\Delta\phi + \delta$ , where  $\delta$  is the random error. As the antenna separation D increases, the minimum quantization level for expressing  $\cos\theta$  decreases, leading to a finer resolution in estimating the spatial angle  $\theta$ .

Then, let's return to the general case in Fig. 4b. A hyperbola is defined as the trajectory of a point that has the same distance difference from two fixed points (focal points). Thus,  $\Delta d$  equals  $2a$ , the length of major axis of the hyperbola. In the case of  $\Delta\phi$  known, all possible positions of S are on one of the hyperbolas with fixed  $k$ . Hence, all possible positions of S constitute a hyperbolic family.

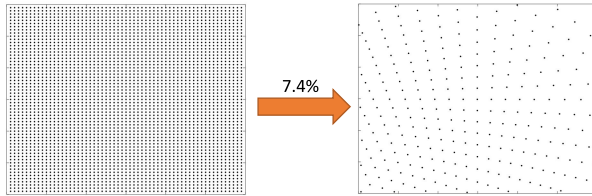


Fig. 5. *Naive hologram and selective hologram*: The left graph shows the naive hologram of size  $3\lambda \times 3\lambda$  with each grid of size  $0.05\lambda \times 0.05\lambda$ . The right one shows selective hologram with candidate points when we intersect the hyperbolas, which has only 7.4 percent of points of the corresponding naive hologram, greatly reducing computation complexity.

In fact, the aforementioned ray is the asymptote of the hyperbola with the same  $k$ . Therefore, the ray model is an approximation of the hyperbola model, which is imprecise in the near situation. Similarly, as  $D$  increases, the ambiguity and the resolution goes up at the same time.

### 3.2 Selective Hologram

Intuitively if we want to improve the accuracy of the trajectory, we should choose the high-resolution scheme, antenna pairs with wide separation. Unluckily, high resolution is always accompanied by high ambiguity. With an antenna pair, the tag will be located at a family of hyperbolas. Easily, intersecting the hyperbolas of two perpendicular pairs, the intersections named candidate points will be the possible locations of the tag. Fig. 3a shows the procedure. The size of the square is  $4\lambda \times 4\lambda$  and about one thousand candidates will be obtained by intersection. In the following sections, voting will be used to eliminate ambiguity to get an initial position.

*Antenna Placement Comparison.* Both RF-Pen and RF-IDraw [5] use 4 antennas, but different antenna setups lead to different resolutions. Fig. 3b shows the setup of RF-IDraw and its candidate points obtaining procedure. At the horizontal direction, the antenna pair with a  $4\lambda$  separation emits a set of hyperbolas, just like RF-Pen. But at the vertical direction, the antenna pair with a  $\frac{\lambda}{8}$  separation emits a thick hyperbola. Therefore, the resolution of RF-IDraw is much lower than RF-Pen, resulting in lower trajectory accuracy.

*Selective Hologram.* After all the candidate points are obtained, we assign equal weight to all the points as default values and call it selective hologram. This selective hologram not only has fine-resolution beams but also largely reduces point compared to a naive hologram. To get a feel of how much it can do, a concrete example is given in Fig. 5. It's

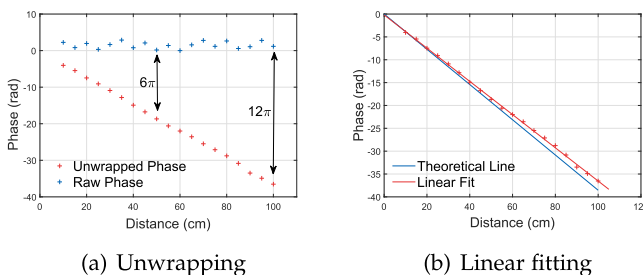
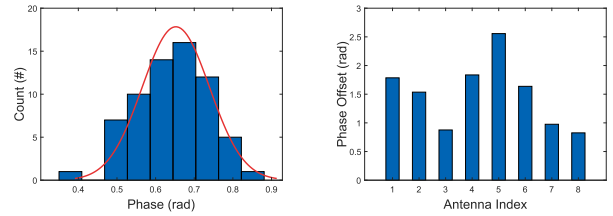


Fig. 6. *The relationship between phase and distance*: (a) This subgraph shows the unwrapping procedure: Each point is subtracted by an integer multiple of  $\pi$ . (b) When the phase is unwrapped, it's linear with the distance. Moreover, it's close to the theoretical line, which represents that phase is a good measure of distance.



(a) The distribution of phase (b) The phase offsets of different antennas

Fig. 7. *Phase error*: This figure shows the errors of the phase. (a) Although the antenna and tag are both stationary, the phase is still not a stable value due to  $\delta$ . The red line is a Gaussian distribution, and the phase distribution is basically consistent with it. Therefore, the random error  $\delta$  obeys a Gaussian distribution with a mean of 0. (b) Phase offset  $\phi_0$  is introduced by hardware and differs from antenna to antenna. The difference between maximum and minimum is more than  $\frac{\pi}{2}$ , which can't be ignored. To get a more precise location, we will calibrate it later.

worth noting that RF-Pen can still track accurately outside of the square as long as within the working range of RFID.

## 4 PHASE-BASED VOTING

After obtaining the selective hologram, the major task is how to pick up the right initial position from it, i.e., removing ambiguity. In this section, we present how to use *phase* measurements to help choose the initial position.

### 4.1 Phase

Equation (1) shows that the unwrapped phase is linear with distance. However, errors are ignored in this simple equation. Considering errors, the phase can be expressed as follows

$$\phi = \left( -\frac{4\pi d}{\lambda} + \phi_0 + \delta \right) \bmod \pi, \quad (5)$$

where  $\phi_0$  is the phase offset introduced by hardware interface,  $\delta$  is the random error. Our experiment confirms the linear relationship. We fix the position of the antenna, move the tag from 10 cm to 100 cm away, and measurement is performed every 5 cm. Every measurement lasts 30 seconds and the mean phase is marked at Fig. 6a. Then, we unwrap every point by subtracting an integer multiple of  $\pi$ . The unwrapped phase has good linearity, so we linearly fit it in Fig. 6b. The fitting line is very close to the theoretical line, signifying that phase is a good measure of distance.

However, the phase information is derived from the signal, which inevitably carries thermal noise from the reader, leading to a random error. We measured hundreds of phase conditions for different channels (from 920,625 to 924,375 kHz, 16 channels), different distances (from 10 to 100 cm), and different antennas (8 antennas), one of which is shown in Fig. 7a. Experiments show that the random error is a Gaussian distribution with a standard deviation of about 0.1 rad. Obviously, such a large random error is harmful to our positioning and tracking.

The phase offset introduced by the hardware is also one of the significant parts. In RF-Pen, both reader and tag are unique, but the antennas and ports are not. Luckily, there is no phase offset between the received signals on today's commercial RFID reader's ports, which is confirmed by our experiment. However, we validate the existence of antenna's

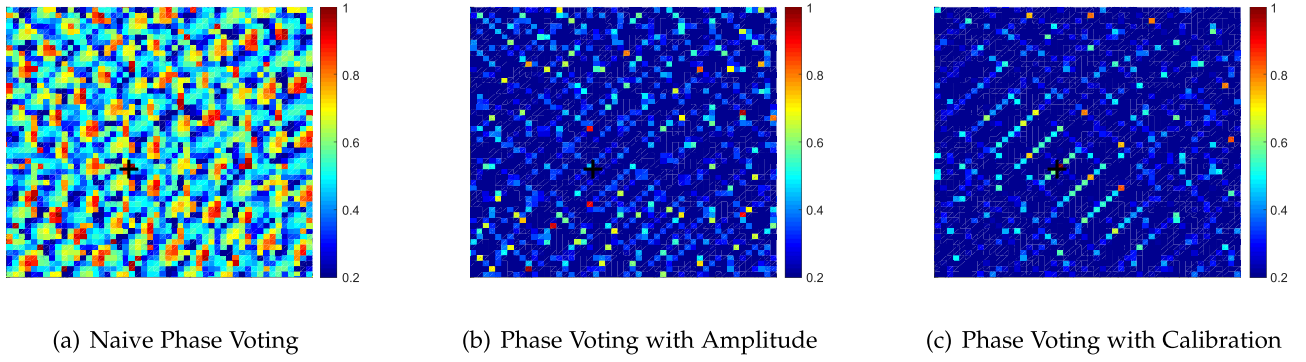


Fig. 8. *Phase voting models*: The black cross mark symbols the groundtruth. (a) We do nothing with phase errors and there are red grids nearly everywhere. (b) We weight the votings to weaken the impact of  $\delta$ . Red areas shrink but become far away from the groundtruth. (c) After calibration, we eliminate the effect of  $\theta_0$  and a red grid is near the groundtruth. However, many red grids far away from the groundtruth exist so that it's hard to choose the proper one.

diversity on the RF phase. By linearly fitting the distance-phase plots of the different antennas, we obtain the offset of each antenna. Fig. 7b shows the difference in the offset of antennas. The values of offsets are not consistent, and the two with the largest deviation exceed  $\frac{\pi}{2}$ . Obviously, the existence of such deviations would affect the positioning and tracking accuracy severely.

## 4.2 Calibrations in Phase Voting

To choose a proper initial position, RF-Pen also uses voting just like RF-IDraw. By voting, the candidate near the groundtruth has a high voting while others have a low voting. Thus, we can easily choose the proper candidate point.

We suppose that  $m$  is the number of antennas and the reader takes only one round of antenna schedule. Thus, there are  $m$  phase values which can be arranged as a vector

$$\Phi = (\phi_1 \quad \phi_2 \quad \dots \quad \phi_m).$$

*Naive Phase Voting (NPV)*. There is a simple thought about voting: For every candidate, calculate the theoretical phase and make a difference with the actual one. Ignoring all errors, the difference can be expressed as

$$h(\mathbf{P}, \mathbf{A}, \phi) = \left( -\frac{4\pi}{\lambda} \|\mathbf{P} - \mathbf{A}\| - \phi \right) \bmod \pi, \quad (6)$$

where  $\mathbf{P}$  is the location vector of the candidate point,  $\mathbf{A}$  is the location vector of an antenna,  $\phi$  is the actual phase value the antenna measured. Considering that phase values are wrapped by  $\pi$ , the difference  $h$  should also be wrapped.

To get the voting of a candidate point, we should combine  $h$  of all antennas. The voting of a candidate point can be defined as follows

$$V(\mathbf{P}) = \left| \sum_{i=1}^m e^{2Jh(\mathbf{P}, \mathbf{A}_i, \phi_i)} \right|, \quad (7)$$

where  $J$  is the imaginary unit. So,  $e^{2Jh}$  represents a complex exponential signal with unit amplitude. Because  $f(x) = e^{Jx}$  is a function with period  $2\pi$ , the factor 2 is necessary.

On the one hand, if the candidate point is near the groundtruth,  $h$  is nearly 0 with all antennas. Therefore,  $V$  will be at a high level. On the other hand, other candidates'  $h$

is ranged in  $(0, \pi)$ , different  $e^{2Jh}$  will cancel each other leading to a low  $V$ . Fig. 8a shows the result of NPV. The votings have been normalized. *For better illustration, unless specified, all grids are voted instead of candidate points for the rest of this paper. In practice, only candidate points need to be voted.*

From the figure, we can discover that red grids exist nearly everywhere. We can hardly pick up a proper candidate using NPV.

*Phase Voting With Amplitude (PVA)*. The failure in NPV forces us to focus on errors. In NPV, the amplitudes of all signals are uniformly set to one. We hope the different  $e^{2Jh}$  will cancel each other when the point is not correct, but it doesn't work well. Now, we have an idea to weight the amplitudes according to the possibility of being the true position instead of uniformly setting to one.

In fact, there is a random error in phase value, which obeys Gaussian distribution as aforementioned. Suppose the tag is at  $\mathbf{P}$ , the phase measured by antenna at  $\mathbf{A}$  has a random error  $\delta$ . Therefore, as the difference between the theoretical and practical value,  $h$  has the same error. In Equation (5),  $\delta \sim \mathcal{N}(0, 0.1)$ . Thus,  $\mu = 0$  and  $\sigma = 0.1$  will be adopted in following sections. The voting of a candidate point can be expressed as follows

$$V(\mathbf{P}) = \left| \sum_{i=1}^m W_i e^{2Jh(\mathbf{P}, \mathbf{A}_i, \phi_i)} \right|$$

$$W_i = 2 \times F(\min\{h(\mathbf{P}, \mathbf{A}_i, \phi_i), \pi - h(\mathbf{P}, \mathbf{A}_i, \phi_i)\}; 0, 0.1) \quad (8)$$

$$F(x; \mu, \sigma) = \frac{1}{\sqrt{2\pi}\sigma} \int_x^\infty \exp\left(-\frac{(t-\mu)^2}{2\sigma^2}\right) dt.$$

Intuitively, the amplitude is the probability that error is larger than  $h$ . Fig. 8b shows the result of PVA. The red areas are much smaller than NPV, but still, too many red grids exist. What's worse, there is no red grid near the groundtruth which means it's impossible to pick up a proper grid.

*Phase Voting With Calibration (PVC)*. No red grid near the groundtruth is a fatal problem. By reviewing Equation (5), we find initial offset  $\phi_0$  is ignored. Due to the existence of  $\phi_0$ ,  $h$  will be  $\phi_0$  rather than 0 in the correct position.  $\phi_0$  is determined by hardware interface and values randomly so that a severe self-cancel-out happened to result in a low voting. Therefore, we do need a countermeasure.

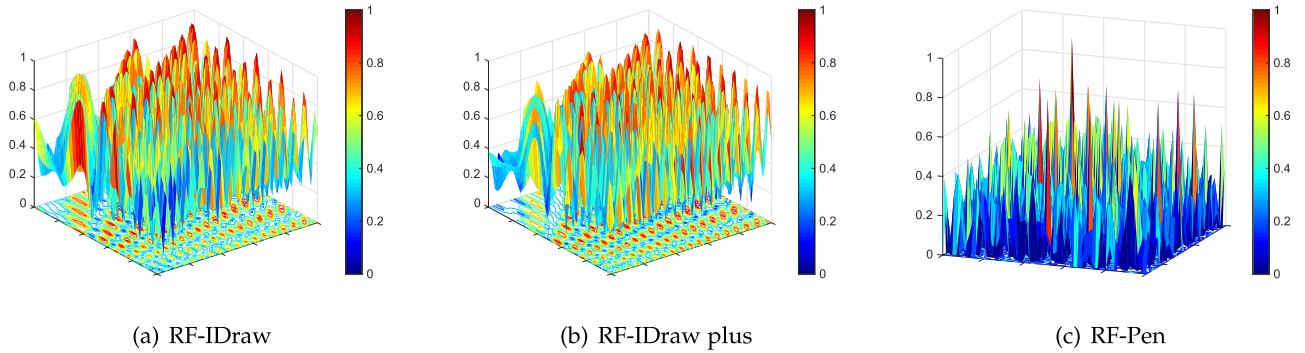


Fig. 9. *Voting comparison between RF-IDraw and RF-Pen*: This figure shows the comparison based on phase. (a) RF-IDraw ignores the Gaussian distribution of phase. Thus, there are too many peaks to find a proper initial position. (b) Even if a calibration is finished to eliminate the effect of  $\phi_0$ , little improvement can be found in RF-IDraw. (c) In RF-Pen, only several peaks exist and one is much higher than the others. Obviously, RF-Pen's result is much better than RF-IDraw's.

A static calibration can be used to solve this problem. There is a linear relationship between phase and distance, and the slope is known. Therefore, only one equation is needed to solve the line. Put the tag stationarily at a known place and measure the mean phase for every antenna, we can easily get the phase offsets of all antennas. Fortunately, if we don't change the antenna setup, calibration should only be done once.

Fig. 8c shows the result of PVC. Just like PVA, there are still many red grids. But only one red grid is near the groundtruth. It is significant progress over NPV and PVA.

### 4.3 Summary

In the last subsection, we explored the mechanism for phase-based voting in detail. Unfortunately, in spite of making full use of the various properties of the phase, we can't effectively reduce the ambiguity and choose a proper initial position. Therefore, simply utilizing phase is not a viable path, which motivates us to combine phase-based voting with other methods.

*Comparison With RF-IDraw.* Though RF-Pen's phase-based voting itself can not reduce ambiguity well, it's much better than RF-IDraw's voting. Fig. 9 shows the voting comparison between RF-IDraw and RF-Pen based on phase. RF-IDraw regards the phase as a stable value, not a Gaussian distribution variable. Thus, it can not eliminate the effect of  $\delta$  and its heat map is like NPV in some degree. Even if the calibrated phase values are put into RF-IDraw, the heat map has not changed substantially. In short, RF-Pen reduces ambiguity much more effectively than RF-IDraw.

## 5 RSSI-BASED VOTING

In the last section, we observed that the phase-based voting cannot effectively reduce all ambiguity. We here ask whether RSSIs can be effectively used for voting and help reduce ambiguity. The answer is Yes.

### 5.1 RSSI

Received Signal Strength Indicator is a common parameter that RFID systems support. The unit of RSSI can be  $dBm$ , which characterizes energy intensity. It can be modeled as follows [9]

$$P'[dBm] = 10\lg P[mW], \quad (9)$$

where  $P'$  is power in  $dBm$  while  $P$  is power in  $mW$ .

In space, energy decays exponentially. The longer the distance experienced, the lower the energy. RSSI is a function of distance to the  $n$  power

$$RSSI[mW] \propto \left(\frac{d}{d_0}\right)^n, \quad (10)$$

where  $n$  is an exponent depicting the rate of energy decay,  $d_0$  is a reference distance and  $d$  is the reader-tag distance. When plotted on a log-log scale, the relationship between RSSI and distance is linear. With the unit  $dBm$ , RSSI is expressed as

$$RSSI = RSSI_0 + 10 \times n \times \lg\left(\frac{d}{d_0}\right), \quad (11)$$

where  $RSSI_0$  is the RSSI at the reference distance. The factor  $n$  is determined as a function of general surroundings. Fig. 10 shows the relationship between RSSI and distance. The linearity of the RSSI is far worse than the phase, but it can still be a good metric of distance.

A one-time calibration is used to determine  $d_0$  and  $RSSI_0$ . We set  $d_0 = \frac{\lambda}{2}$  and place the tag  $\frac{\lambda}{2}$  away from an antenna. We keep the tag stationary and record RSSI for 1 min, regarding the mean as  $RSSI_0$ . These values will be effective in one experimental period.

### 5.2 Calibrations in RSSI Voting

In a round of communication between the reader and tag, one phase value and one RSSI value are received at the

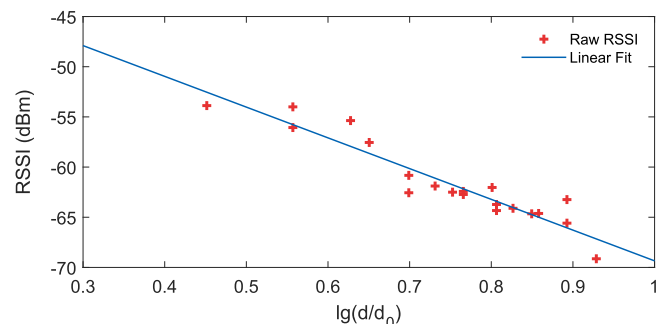


Fig. 10. *The relationship between RSSI and distance*: When we take the logarithm of the distance, the RSSI has a linear relationship with it. Though the error is a bit large, RSSI can still be a good metric for positioning.

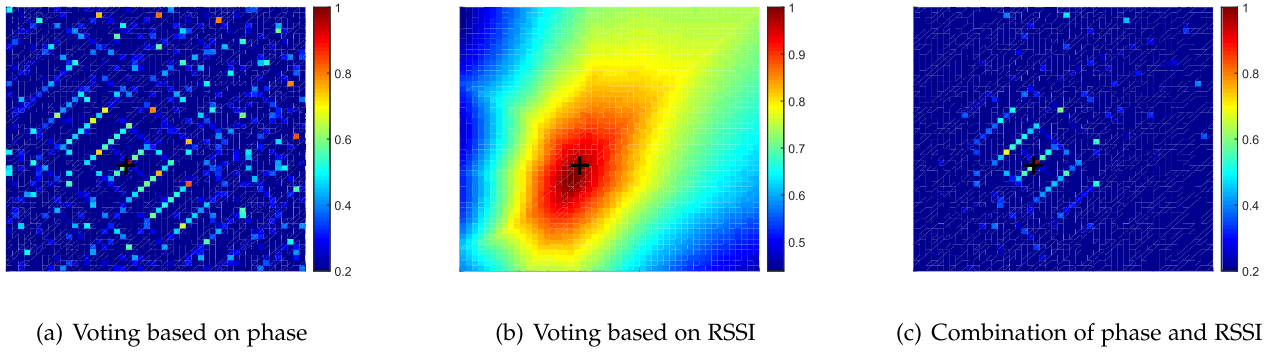


Fig. 11. *Hybrid Voting*: The black cross denotes the groundtruth. (a) and (b) are the original voting. (c) Combining RSSI-based and phase-based voting, the point closest to the groundtruth has the highest likelihood. Moreover, points with high votings are distributed around the groundtruth.

same time. Thus, similarly as phase, there are  $m$  RSSI values. Meanwhile,  $RSSI_0$  will also be used. There is a vector

$$\mathbf{RSSI} = (RSSI_0 \quad RSSI_1 \quad RSSI_2 \quad \dots \quad RSSI_m).$$

According to Equation (11), we can get an equation as follows

$$RSSI - RSSI_0 = 10 \times n \times \lg\left(\frac{d}{d_0}\right). \quad (12)$$

Normally,  $n$  is determined as a function of surroundings, independent of antennas. Therefore, if we divide the Equation (12) for two different antennas, we can eliminate  $n$ .

$$\frac{RSSI_i - RSSI_0}{RSSI_j - RSSI_0} = \frac{\lg(d_i/d_0)}{\lg(d_j/d_0)}, \quad (13)$$

where  $RSSI_i$  is the actual RSSI value of antenna  $i$ ,  $RSSI_0$  is the RSSI value at the reference distance,  $d_i$  is the distance from antenna  $i$  to the tag. For known locations, the left side of the equation can be calculated from the right side. Thus, for every candidate point, we can compare the theoretical value of  $\frac{RSSI_i - RSSI_0}{RSSI_j - RSSI_0}$  with actual value and take a vote.

Based on Equation (13), the voting of a candidate point from antenna pair  $\langle i, j \rangle$  can be expressed as follows

$$V_{ij}(\mathbf{P}) = \min\left\{\frac{R_{ij}}{T_{ij}(\mathbf{P})}, \frac{T_{ij}(\mathbf{P})}{R_{ij}}\right\} \quad (14)$$

$$R_{ij} = \frac{RSSI_i - RSSI_0}{RSSI_j - RSSI_0}$$

$$T_{ij}(\mathbf{P}) = \frac{\lg(\|\mathbf{P} - \mathbf{A}_i\|/d_0)}{\lg(\|\mathbf{P} - \mathbf{A}_j\|/d_0)}.$$

Obviously, the closer theoretical and actual values are, the higher the voting. The total voting of a candidate is the sum of all antenna pairs.

$$V(\mathbf{P}) = \sum_{i=1}^{m-1} \sum_{j=i+1}^m V_{ij}(\mathbf{P}). \quad (15)$$

Fig. 12 shows the complete process of RSSI-based voting. With the effort of every antenna pair, only the area close to the groundtruth is red. But the area is a bit large, due to the low resolution. In fact, the RSSI-based voting depends on the quality of RSSI, which will be discussed in the next section.

In Section 2, we had a conclusion: The tracking accuracy will be acceptable as long as the initial positioning error is not large. Therefore, we can use it as a filter to reduce ambiguity. Even if there are several candidate points in the red area with confusion, the initial position will not be distant from the groundtruth.

## 6 HYBRID VOTING

Now we have two voting methods. One is based on phase and the other is based on RSSI. The RSSI-based voting limits the candidates in an area close to the groundtruth, while the phase-based voting limits them in a few points. Therefore, we should make hybrid voting of the two. By leveraging the advantages of both, we can create better voting.

A simple combination is a linear synthesis, which can be expressed as follows

$$V_c(\mathbf{P}) = \alpha \times V_p(\mathbf{P}) + (1 - \alpha) \times V_R(\mathbf{P}), \quad (16)$$

where  $\alpha \in [0, 1]$  is the linear parameter. When  $\alpha = 0$ , it is purely RSSI-based voting; When  $\alpha = 1$ , it is purely phase-based voting.

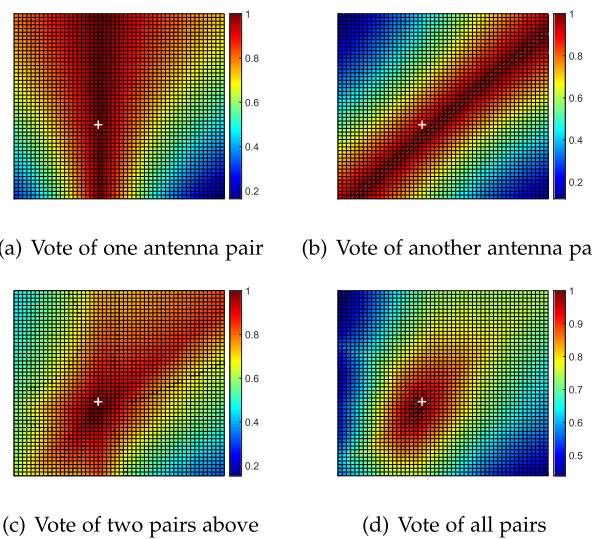


Fig. 12. *RSSI-based voting model*: These four subgraphs show the complete progress of voting with RSSI. The white cross mark symbols the groundtruth. (a) Voted by a pair of antennas, the red area is a strip shape. (b) Voted by another pair of antennas, another strip zone has a high likelihood. (c) By putting the above votings together, the intersection has a high probability. (d) Using all of the antenna pairs to evaluate, we have succeeded in narrowing the high probability area.

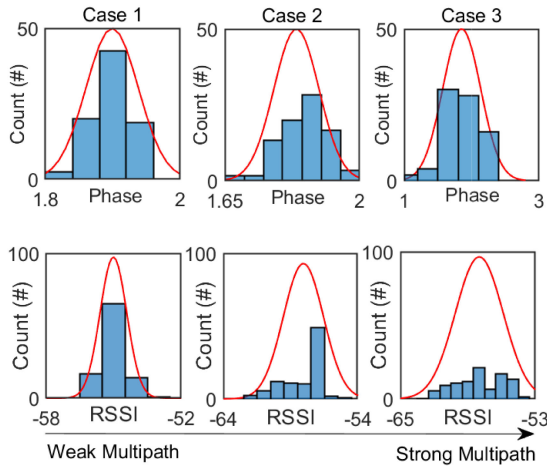


Fig. 13. *Phase and RSSI Quality Comparison*: These graphs show the phase and RSSI distribution in different multipath conditions. As the multipath strengths, the variance of the phases increases and the RSSI becomes less stable.

We set an experiment under different multipath conditions to find the proper  $\alpha$ . Fig. 13 shows the phase and RSSI distribution of a stationary tag in these cases. We calculate the mean and variance and fit them with Gaussian distribution (the red line). Under different multipath conditions, phase and RSSI shows different qualities. As a result, the weak multipath leads in stable and consistent Gaussian distributed phase/RSSI, which is called high-qualified phase/RSSI.<sup>1</sup>

To select the proper  $\alpha$ , in each case, we place the tag at about 50 randomly selected places stationarily for more than 10 seconds and record the locations. The euclidean distance between the groundtruth and the predicted position is regarded as the initial position error. We traverse  $\alpha$  and the result is shown in Fig. 14.

- Hybrid voting combines the advantages of RSSI-based voting and phase-based voting as shown in Fig. 11. With a proper  $\alpha$ , its results are better than both of them. In these three cases, hybrid voting is  $1.16\times$ ,  $1.35\times$  and  $1.50\times$  better than RSSI-based voting,  $4.19\times$ ,  $2.54\times$  and  $1.55\times$  better than phase-based voting.
- In different multipath conditions, the proper ranges of  $\alpha$  are different. It's  $0.25 \pm 0.25$ ,  $0.3 \pm 0.1$  and  $0.7 \pm 0$  in those three cases. Thus, there is a trend that  $\alpha$  increases when the multipath strengthens. Because the accuracy of phase-based voting is stable with the increasing multipath while the accuracy of RSSI-based voting decreases rapidly.
- $\alpha$  should be adjusted with different multipath conditions. With strong multipath, we can use a machine learning method based on a large data set, which is left as our future work. As for weak multipath,  $\alpha$  is insensitive over a wide range. Therefore, RF-Pen is recommended to be used in the weak multipath case, such as LOS situation with a dominating direct path.

*Theoretical Analysis.* Take Case 1 for example, the standard deviation of phase measurement is  $0.1\text{rad}$ , which corresponds to  $0.5\text{ cm}$  error according to Eq. (1). But the

1. The experiments in Section 8 were conducted with high-qualified RSSI without specific notes.

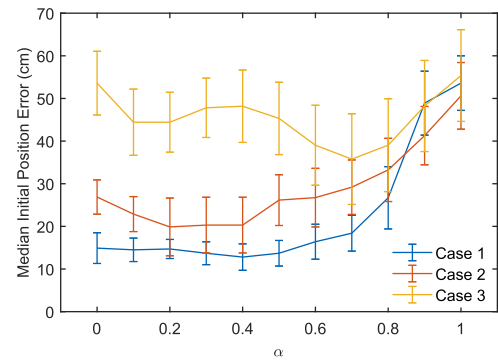


Fig. 14. *The proper linear parameter*: In order to make the overall evaluation more accurate, we traverse  $\alpha$  in step size 0.1 to find a proper parameter  $\alpha$  for each case.

ambiguity may lead to an additional error of several wavelengths. As for RSSI, Eq. (11) shows the theoretical formula and Fig. 13 illustrates that RSSI measurement error is about  $2\text{ dBm}$ . Table 2 shows the position error from a single antenna's RSSI at different distances. Combining phase and RSSI measurement from multiple antennas, the position error will be lower. Moreover, Section 8.3 shows the relationship between initial position error and trajectory error. Theoretically, the median trajectory error will be about  $2\text{ cm}$ .

## 7 IMPLEMENTATION

With commercial off-the-shelf RFID readers, we built a prototype of RF-Pen. It can trace the trajectory of EPC Gen-2 UHF tags, and display the trajectory in real-time.

*Hardware.* We use a ThingMagic M6e 4-port UHF RFID reader without any hardware or firmware modification, which connects 4 antennas. The UHF RFID tag is kept parallel to the polarization direction of the antennas.<sup>2</sup> With a carrier frequency of  $920\text{ MHz}$ , the reader continuously queries the tag and sends the phase and RSSI values to a PC running RF-Pen program via a data cable. The antenna setup is shown in Fig. 3a. The size of the square is  $4\lambda \times 4\lambda$ . Three antennas locate at the corners of the square, and the other one locates at the midpoint of the bottom edge.

*Software.* The RF-Pen program is implemented using Java together with official Mercury APIs. All the phase and RSSI measurements are obtained in real-time. Meanwhile, we design a simple GUI to help using RF-Pen.

*Trajectory Tracking.* The tracing works by tracking the beams of the chosen initial position, which is inspired by RF-IDraw. This process is iteration-based. In every iteration, RF-Pen obtains candidates as shown in Section 3. From these candidates, RF-Pen selects the one closest to the position in the last iteration as the position in this iteration. To reduce computational complexity, RF-Pen looks for the hyperbola whose argument  $a$  is the closest to the last iteration in both directions. Then, the intersection of hyperbolas is regarded as the position in this iteration. Therefore, RF-Pen iteratively determines all the positions on the trajectory.

*Competitors.* We reproduced RF-IDraw according to the detailed instructions in paper [4]. It should be noted that

2. According to [10], it's equivalent to only allow the tag's rotation along Z axis. The influence is so weak that can be handled as noises.

TABLE 2

The Theoretical Position Error From RSSI at Different Distances

Distance (cm)	30	60	90	120	150
RSSI (dBm)	-48.0	-57.1	-62.3	-66.1	-69.0
Position Error (cm)	4.60	9.21	13.82	18.42	23.0

distance needs to be doubled due to the round trip of the electromagnetic wave (In fact, RF-IDraw mentions this in a footnote). The performance of ours is similar to that shown in paper [4]. In Section 8, we compare RF-Pen with 4-antenna RF-IDraw and 8-antenna RF-IDraw in initial position accuracy and trajectory accuracy. They are built using the same devices as RF-Pen. The antenna setup of 4-antenna is shown in Fig. 3b. To ensure the beam of narrow-separation antenna pair is unique, the separation of the antenna pair is set to  $\frac{\lambda}{8}$ . The antenna setup of 8-antenna RF-IDraw is shown as follows. Just like RF-Pen, there is a  $4\lambda \times 4\lambda$  square. Four antennas are placed at the corners of the square, connected to one reader. At the middle of the left edge and bottom edge, two antenna pairs with  $\frac{\lambda}{8}$  separation are placed, connected to the other reader.

## 8 EVALUATION

### 8.1 Initial Position Accuracy

We first test the initial position accuracy of RF-Pen. Fig. 15a shows CDF for initial position error for RF-Pen and 4-antenna and 8-antenna RF-IDraw. The median initial position error of RF-Pen is 12.8 cm, and the 90th percentile is 30.3 cm. In contrast, the accuracy of RF-IDraw is far less than that. RF-Pen's median initial position accuracy is  $2.9\times$  better than 8-antenna RF-IDraw and  $4.1\times$  better than 4-antenna RF-IDraw.

Fig. 15b shows CDF for initial position error for RF-Pen using phase-based voting and hybrid voting. Using phase-based voting only, the median initial position error is 53.6 cm and hybrid voting is  $4.2\times$  better than phase-based voting.

- The initial position accuracy is determined by two important factors: candidate quality and ambiguity. First, since the phase of RF-IDraw isn't calibrated, the candidate points of RF-IDraw drift leading to low quality. Second, in RF-Pen, the RSSI-based voting has low resolution but no ambiguity, thus the initial

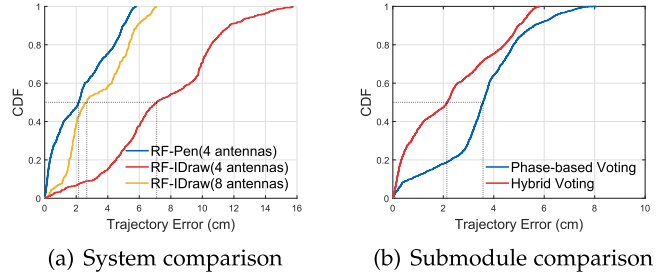


Fig. 16. *Trajectory accuracy*: (a) This subgraph shows the accuracy of RF-Pen and RF-IDraw in trajectory tracking. The median accuracy of RF-Pen is 2.15 cm,  $3.3\times$  better than RF-IDraw with 4 antennas. Moreover, it's even slightly better than RF-IDraw with 8 antennas. (b) This subgraph shows the accuracy of RF-Pen in trajectory tracking using phase-based voting and hybrid voting. Hybrid voting is significantly better than phase-based voting.

position will not be far away from the groundtruth. In RF-IDraw, however, the phase offset is not calibrated so that the beam of narrow-separated pair may deviate seriously from the groundtruth. Therefore, it's not surprising that RF-Pen's initial position accuracy is much better than 8-antenna RF-IDraw.

- As discussed in Section 4, phase-based voting can not reduce ambiguity well so that the accuracy is low. With the help of RSSI-based voting, our hybrid voting takes advantage of these two methods and achieves the best accuracy.

### 8.2 Trajectory Accuracy

Then, we test the trajectory accuracy of RF-Pen. We move the tag along with the rectangular trajectory and track it, then compare the gap between the reconstructed trajectory and the groundtruth. In order to eliminate the influence of initial offset, we pan the reconstructed trajectory until its centroid coincides with the centroid of the groundtruth. After that, we calculate the point-to-graphic distance between the point in the reconstructed trajectory and that in the groundtruth as the trajectory error.

Fig. 16a shows CDF for trajectory error for RF-Pen and 4-antenna and 8-antenna RF-IDraw. The median trajectory accuracy of RF-Pen is 2.15 cm, and 90th percentile is 4.98 cm. Its median accuracy is  $3.7\times$  better than 4-antenna RF-IDraw. Even if 8-antenna RF-IDraw has twice the antenna, RF-Pen still achieves slightly better accuracy than it.

Fig. 16b shows CDF for trajectory error for RF-Pen using phase-based voting and hybrid voting. The median trajectory accuracy using phase-based voting is 3.58 cm and hybrid voting achieves a much better accuracy once again.

- 4-antenna RF-IDraw has a large trajectory error. On the one side, it's caused by the big initial position error. On the other side, because of the use of a narrow-separation antenna pair, the resolution of its candidate points are not as high as RF-Pen's. Under the combined effect of the above two reasons, the trajectory accuracy of RF-IDraw is much lower than that of RF-Pen.
- Although RF-Pen is much better than 8-antenna RF-IDraw in initial accuracy, it does not have such a big advantage in trajectory accuracy, which affirms that the initial offset has minimal effect on trajectory

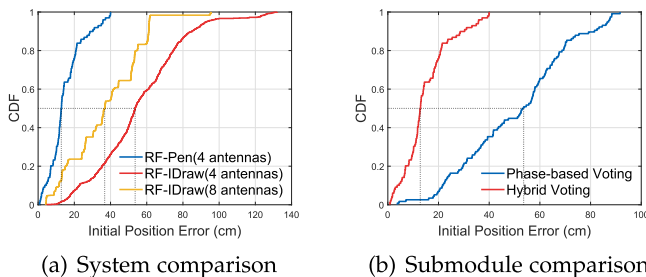


Fig. 15. *Initial position accuracy*: (a) This subgraph shows the accuracy of RF-Pen and RF-IDraw in initial positioning. The median accuracy of RF-Pen is 12.8 cm,  $2.9\times$  better than RF-IDraw with 8 antennas and  $4.1\times$  better than that with 4 antennas. Meanwhile, the 90th percentile of RF-Pen is 30.3 cm, even smaller than RF-IDraw's median accuracy. (b) This subgraph shows the accuracy of RF-Pen in initial positioning using phase-based voting and hybrid voting. Hybrid voting is much better than phase-based voting.

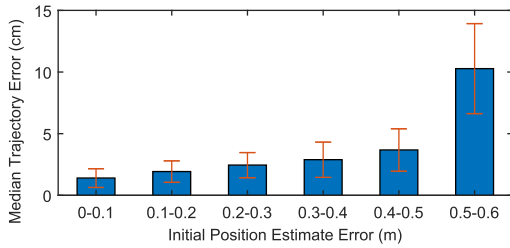


Fig. 17. *The effect of initial position accuracy on trajectory accuracy:* Initial position accuracy and trajectory accuracy are positively correlated. However, if the initial position error is within 50 cm, the trajectory accuracy is acceptable. Luckily, even the 90th percentile of RF-Pen is just 30.3 cm, far less than 50 cm.

accuracy as long as the initial position error is within an acceptable range.

- The trajectory accuracy difference of RF-Pen using different voting methods is mainly caused by initial position accuracy, which is why hybrid voting outstands phase-based voting.

### 8.3 The Effect of Initial Position Accuracy on Trajectory Accuracy

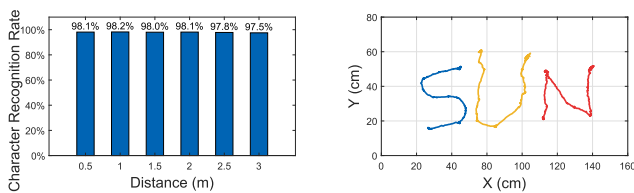
As shown in Fig. 2, the trajectory accuracy will be acceptable as long as the initial position error isn't too large. Here we conduct detailed experiments to examine this point further. When tracking the tag, we can manually specify the initial point and track it. Obviously, different initial points lead to different trajectories. Grouping the trajectories according to their initial position error, we calculate the trajectory error for each trajectory.

The result is shown in Fig. 17.

- Initial position accuracy and trajectory accuracy are positively correlated, which is in line with our expectations. The closer to the groundtruth, the less the distortion of the trajectory.
- As long as the initial position error is within 50 cm, the trajectory error will be acceptable. From the figure, the trajectory error rises steadily when the initial position error is less than 50 cm. But after that, the trajectory error rockets up.

### 8.4 Character Recognition Application

To prove the feasibility of an RF-based virtual touch screen, we use the prototype of RF-Pen in character recognition. A



(a) Character recognition (b) Reconstructed trajectory

Fig. 18. *Character recognition:* (a) This subgraph shows the character recognition success rate of RF-Pen at different distances. When the distance from the user to antennas varies from 0.5 m to 3.0 m, the success rate is maintained at a high value. When the distance is greater than 2 m, the success rate drops slightly. (b) This subgraph shows the reconstructed trajectory of the written word 's', 'U', 'N'. The trajectory tracked by RF-Pen is clear and easy to recognize.

TABLE 3  
Time Delay of Different Systems per Round

Delay	RF-Pen	RF-IDraw	Tagoram
Reading	140 ms	280 ms / 2.0×	140 ms / 1.0×
Computing	9 us	3 us / 0.33×	1896 ms / 2.1E5×
Total	140 ms	280 ms / 2.0×	2036 ms / 15×

user writes characters in the air and RF-Pen tracks his writing trajectory and records it. The width of the user's handwritten character is about 20 cm. Then, the script implements a mouse movement event based on the reconstructed trajectory and writes the trajectory to the handwriting recognition area of Sogou Input Method. By calculating the ratio of correct characters in total characters, we can get the character recognition success rate.

Fig. 18a shows the character recognition success rate in different distance between the user and the antennas. As we can see, from 0.5 m to 3 m, the success rate is all around 98 percent. The total character recognition success rate is 97.9 percent. Fig. 18b shows the reconstructed characters. They are clear and easy to recognize, which means that the virtual touch screen is feasible.

- RF-Pen has an advantage in character recognition. Although the median trajectory error is 2.15 cm, the error is caused by the enlarging of the trajectory, not randomly distributed. Therefore, the features of the character will not be destroyed during reconstruction, which is favorable for character recognition. In fact, the characters written by different people are not exactly the same, which can be handled naturally by the character recognition program.
- At different distances, the recognition rate is basically unchanged. The reason is that the trajectory error is mainly caused by the trajectory enlarging even when the distance is large, which can be treated by the character recognition program.

### 8.5 Real-Time Performance

To evaluate the real-time performance of RF-Pen, we measure the time cost of reading and computing. Comparing with 8-antenna RF-IDraw and Tagoram with unknown track, the mean delay is shown in Table 3. The total delay per round of RF-Pen is only 140 ms, which is 2× faster than RF-IDraw and 15× faster than Tagoram. All in all, RF-Pen provides a real-time trajectory tracking.

- In RFID systems, tag reading is a major latency due to slow energy harvesting. Therefore, reducing the number of antennas can greatly reduce the time delay. Comparing with RF-IDraw, RF-Pen uses only half of the antennas to halve the delay.
- For an unknown track, Tagoram compares the PSNR<sup>3</sup> of trajectory starting from different grids. For a single round, the computing complexity is  $O(W^2L^2)$  (The

3. Peak-Signal-to-Noise-Ratio(PSNR) is a metric in Tagoram to evaluate the likelihood that the initial position is at the corresponding grid. To evaluate a trajectory, Tagoram regards the trajectory as known and calculate the PSNR of its initial position. The computation complexity of PSNR is  $O(WL)$  per round.

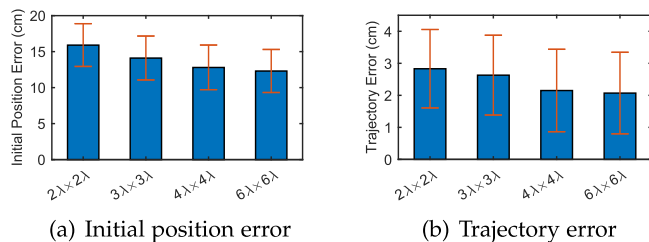


Fig. 19. The accuracy of RF-Pen in different sizes: By scaling the setup, RF-Pen can be set to different sizes. With the shrinking of size, both the initial position accuracy and the trajectory accuracy have dropped, but not much, which demonstrates RF-Pen’s expansibility. In practice, we can choose a proper size according to specific requirements.

plane is divided into  $W \times L$  grids). Thus, computing delay plays a significant role in Tagoram. RF-Pen achieves a much better real-time performance.

### 8.6 Expansibility

As shown in Fig. 3a, RF-Pen’s antennas are placed in a square whose size is  $4\lambda \times 4\lambda$  ( $1.3m \times 1.3m$ ). In fact, by changing the side length of the square, we can get RF-Pen in different sizes. Fig. 19 shows the initial position accuracy and trajectory accuracy of RF-Pen in different sizes. The accuracy is acceptable in all of these sizes. In practice, we can choose a proper size according to specific requirements. We believe that the expansibility of RF-Pen will benefit a lot more potential applications.

- With the reduction in size, the initial position accuracy drops, mainly due to the decreasing resolution of candidate points. As shown in Section 3, antenna pair with smaller separation leads to the lower resolution.
- Trajectory accuracy is influenced by initial position error and candidate point resolution. Obviously, RF-Pen in small size has low initial position accuracy and low candidate point resolution, leading to low trajectory accuracy.

## 9 DISCUSSION

### 9.1 High-Speed Support

In the iteration, RF-Pen’s tracking part regards the candidate point closest to the position in the last iteration as the position in this iteration. It is based on an assumption: the tag cannot move too fast. We can calculate the fastest speed RF-Pen supported roughly. Generally, the distance between adjacent candidate points is 6 cm. The reader uses each antenna to query the tag in turn, which spends about 150ms per round. Thus, we can get the speed as about 20cm/s. Choosing a false point is called drift. When drift occurs, the accuracy of the tracking trajectory will be affected. Obviously, if a tag moves at a higher speed than 20 cm/s, the trajectory will be deformed severely. One way to solve it is to employ  $2\pi$  phase measurements, which currently can only be realized by soft-defined radios, e.g., USRP. And more advanced reading schemes, such as MIMO and concurrent multiple readers, can help too but bring more hardware cost. Another possible solution is to try to extract more information from physical layer signals and we leave this part for future work.

### 9.2 Beam Pattern

In our assumption, the antennas in RF-Pen are all perfectly omni-directional, which is, however, impossible in the practice. In fact, the manufacturers ensure that the beam pattern can be approximated to be omni-directional in its working range. Thus, the impact of imperfect beam pattern can be ignored just as other papers in this field did [11].

## 10 RELATED WORK

*Whiteboard Transcription Systems.* These systems use high-resolution cameras to record the contents on the whiteboard [12], [13], [14]. They work well when the light is sufficient and the camera can capture the whiteboard content directly, for example in the classroom. The deployment should be in advance and it’s unavailable. In contrast, RF-Pen can be deployed easily with 4 antennas on whiteboards of different sizes. Moreover, writing in the air can be handled by RF-Pen, but these systems shoot and process the handwriting left on the whiteboard. Besides, there are some whiteboards based on ultrasound-infrared [15] and laser curtains [16], which requires expensive styluses. In comparison, RFID tags are much cheaper, which cost a few cents for each.

*RFID-Based Positioning and Tracking Systems.* LANDMARC [17] is the first active RFID positioning system. Deploying multiple anchor tags, LANDMARC achieves meter-level accuracy with the k-nearest neighbor algorithm (KNN). Some works using RSSI to estimate the location of tags. PinIt [18] and OTrack [19] uses the multipath profile of each RFID tag to localize RFID tags. Later works such as RF-IDraw [4], Tagoram [6] and PolarDraw [5] utilize fine-grained phase values to locate tags. Motivated by these systems, RF-Pen’s novelty is integrating RSSI and phase to build a high-performance system. Meanwhile, some works increase accuracy with larger bandwidth and tag arrays, which is a different direction with RF-Pen. RFind [7] and TurboTrack [8] works on a bandwidth over 100 MHz with non-commercial USRP. Tagyro [10] and Pantomime [20] attach multiple tags on an object to track its movement. In contrast, RF-Pen based on COTS devices combines phase and RSSI for great tracking accuracy with 4 antennas and one tag.

*Gesture and Activity Recognition Systems.* In this field, many systems based on different principles exist. E-Gesture [21] and RisQ [22] employ the gyroscope and accelerometer to recognize the predefined gestures. However, these systems only support limited gestures and cannot track the fine-grained finger motions. FingerIO [23] and AAMouse [24] are based on voice, but easily be influenced by environmental noise. Besides, some works obtain information from electromagnetic waves. Wisee [3] uses the Doppler effect to extract human motion from WiFi signals, but can only identify a limited number of activities. WiDraw [25] tracks hand motions by measuring the AoA extracted from CSI but requiring 30 neighboring WiFi devices. Allsee [1] is an RFID-based system which relies on predefined gestures and rules. Widar2.0 [26] tracks the movement of human bodies with COTS WiFi, achieving an accuracy of about 0.75m. RIM [27] measures multiple parameters of motions according to the similarity of CSI with a single AP and a hexagonal antenna array. Differently, RF-Pen identifies different motions by tracking the trajectory of a tag, making it easier to expand.

## 11 CONCLUSION

This paper introduces a new 4-antenna trajectory tracking system, RF-Pen, which can be used in the virtual touch screen. To reconstruct highly accurate trajectory, we have presented how to use selective hologram to maximize tracing resolution and reduce computation overhead. Furthermore, hybrid voting has been demonstrated to effectively remove ambiguity brought by high-resolution beams. Such a phase and RSSI combination enables high precision initial position, leading to accurate trajectory reconstruction. Through off-the-shelf device prototyping, we have shown that RF-pen's median initial position error is 12.8 cm and median trajectory error is 2.15 cm, which is significantly better than 4-antenna RF-IDraw and even outperforms 8-antenna RF-IDraw. We believe RF-Pen will inspire a range of practical new applications in wireless sensing and human-computer interactions.

## ACKNOWLEDGMENTS

This work was supported by the NSFC Grant Nos. 61932017 and 61971390, and the Fundamental Research Funds for the Central Universities No. WK2150110013.

## REFERENCES

- [1] B. Kellogg, V. Talla, and S. Gollakota, "Bringing gesture recognition to all devices," in *Proc. 11th USENIX Conf. Netw. Syst. Des. Implementation*, 2014, pp. 303–316.
- [2] N. Kardaris, I. Rodomagoulakis, V. Pitsikalis, A. Arvanitakis, and P. Maragos, "A platform for building new human-computer interface systems that support online automatic recognition of audio-gestural commands," in *Proc. 24th ACM Int. Conf. Multimedia*, 2016, pp. 1169–1173.
- [3] Q. Pu, S. Jiang, and S. Gollakota, "Whole-home gesture recognition using wireless signals," in *Proc. 19th Annu. Int. Conf. Mobile Comput. Netw.*, 2013, pp. 27–38.
- [4] J. Wang, D. Vasishth, and D. Katabi, "RF-IDraw: Virtual touch screen in the air using RF signals," in *Proc. ACM Conf. SIGCOMM*, 2014, pp. 235–246.
- [5] L. Shangguan and K. Jamieson, "Leveraging electromagnetic polarization in a two-antenna whiteboard in the air," in *Proc. 12th Int. Conf. Emerg. Netw. EXperiments Technol.*, 2016, pp. 443–456.
- [6] L. Yang, Y. Chen, X. Y. Li, C. Xiao, M. Li, and Y. Liu, "Tagoram: Real-time tracking of mobile RFID tags to high precision using COTS devices," in *Proc. 20th Annu. Int. Conf. Mobile Comput. Netw.*, 2014, pp. 237–248.
- [7] Y. Ma, N. Selby, and F. Adib, "Minding the billions: Ultra-wideband localization for deployed RFID tags," in *Proc. 23rd Annu. Int. Conf. Mobile Comput. Netw.*, 2017, pp. 248–260.
- [8] Z. Luo, Q. Zhang, Y. Ma, M. Singh, and F. Adib, "3D backscatter localization for fine-grained robotics," in *Proc. 16th USENIX Symp. Netw. Syst. Des. Implementation*, 2019, pp. 765–782.
- [9] S. Y. Seidel and T. S. Rappaport, "914 MHz path loss prediction models for indoor wireless communications in multifloored buildings," *IEEE Trans. Antennas Propag.*, vol. 40, no. 2, pp. 207–217, Feb. 1992.
- [10] W. Teng and X. Zhang, "Gyro in the air: Tracking 3D orientation of batteryless Internet-of-Things," in *Proc. 22nd Annu. Int. Conf. Mobile Comput. Netw.*, 2016, pp. 55–68.
- [11] T. Liu, Y. Lei, Q. Lin, G. Yi, and Y. Liu, "Anchor-free backscatter positioning for RFID tags with high accuracy," in *Proc. IEEE Conf. Comput. Commun.*, 2014, pp. 379–387.
- [12] L. W. He and Z. Zhang, "Real-time whiteboard capture and processing using a video camera for remote collaboration," *IEEE Trans. Multimedia*, vol. 9, no. 1, pp. 198–206, Jan. 2007.
- [13] P. E. Dickson, W. R. Adrion, and A. R. Hanson, "Automatic capture and presentation creation from multimedia lectures," in *Proc. 38th Annu. Front. Educ. Conf.*, 2008, pp. T2A–14.
- [14] R. Y. D. Xu, "A computer vision based whiteboard capture system," in *Proc. IEEE Workshop Appl. Comput. Vis.*, 2008, pp. 1–6.
- [15] Mimioteach interactive whiteboard. [Online]. Available: <https://www.mimio-boards.com/mimio-teach-interactive-system.html>
- [16] Mimioprojector touch projector. [Online]. Available: [https://www.projectorcentral.com/mimioprojector\\_interactive\\_projector\\_review.htm](https://www.projectorcentral.com/mimioprojector_interactive_projector_review.htm)
- [17] L. M. Ni, Y. Liu, Y. C. Lau, and A. P. Patil, "LANDMARC: Indoor location sensing using active RFID," in *Proc. 1st IEEE Int. Conf. Pervasive Comput. Commun.*, 2003, pp. 407–415.
- [18] J. Wang and D. Katabi, "Dude, where's my card? RFID positioning that works with multipath and non-line of sight," in *Proc. ACM SIGCOMM Conf. SIGCOMM*, 2013, pp. 51–62.
- [19] L. Shangguan, Z. Li, Y. Zheng, L. Mo, and Y. Liu, "OTrack: Order tracking for luggage in mobile RFID systems," in *Proc. IEEE Int. Conf. Comput. Commun.*, 2013, pp. 3066–3074.
- [20] L. Shangguan, Z. Zhou, and K. Jamieson, "Enabling gesture-based interactions with objects," in *Proc. 15th Annu. Int. Conf. Mobile Syst. Appl. Serv.*, 2017, pp. 239–251.
- [21] T. Park, J. Lee, I. Hwang, C. Yoo, L. Nachman, and J. Song, "E-Gesture: A collaborative architecture for energy-efficient gesture recognition with hand-worn sensor and mobile devices," in *Proc. 9th ACM Conf. Embedded Netw. Sensor Syst.*, 2011, pp. 260–273.
- [22] A. Parate, M. C. Chiu, C. Chadowitz, D. Ganesan, and E. Kalogerakis, "RisQ: Recognizing smoking gestures with inertial sensors on a wristband," in *Proc. 12th Annu. Int. Conf. Mobile Syst. Appl. Serv.*, 2014, pp. 149–161.
- [23] R. Nandakumar, V. Iyer, D. Tan, and S. Gollakota, "FingerIO: Using active sonar for fine-grained finger tracking," in *Proc. CHI Conf. Hum. Factors Comput. Syst.*, 2016, pp. 1515–1525.
- [24] S. Yun, Y. C. Chen, and L. Qiu, "Turning a mobile device into a mouse in the air," in *Proc. 13th Annu. Int. Conf. Mobile Syst. Appl. Serv.*, 2015, pp. 15–29.
- [25] L. Sun, S. Sen, D. Koutsonikolas, and K. H. Kim, "WiDraw: Enabling hands-free drawing in the air on commodity WiFi devices," in *Proc. 21st Annu. Int. Conf. Mobile Comput. Netw.*, 2015, pp. 77–89.
- [26] K. Qian, C. Wu, Y. Zhang, G. Zhang, Z. Yang, and Y. Liu, "Widar2.0: Passive human tracking with a single Wi-Fi link," in *Proc. 16th Annu. Int. Conf. Mobile Syst. Appl. Serv.*, 2018, pp. 350–361.
- [27] C. Wu, F. Zhang, Y. Fan, and K. Liu, "RF-based inertial measurement," in *Proc. ACM Special Interest Group Data Commun.*, 2019, pp. 117–129.



**Haoyu Wang** is currently working toward the undergraduate degree from the School of Computer Science and Technology, University of Science and Technology of China, China. His research interests include wireless networks and the Internet-of-Things applications.



**Wei Gong** (Member, IEEE) received the BS degree from the Department of Computer Science and Technology, Huazhong University of Science and Technology, China, the MS degree from the School of Software, Tsinghua University, China, and the PhD degree from the Department of Computer Science and Technology, Tsinghua University, China. He is currently a professor with the School of Computer Science and Technology, University of Science and Technology of China, China. His research interests include backscatter communication, distributed computing, and the Internet-of-Things applications.

▷ For more information on this or any other computing topic, please visit our Digital Library at [www.computer.org/csdl](http://www.computer.org/csdl).